[18F]-FDG PET neuroimaging in rats with quinpirole-induced checking behavior as a model for obsessive compulsive disorder

[^{18}F]-FDG PET neuroimaging in rats with quinpirole-induced checking behavior as a model for Obsessive Compulsive Disorder

Stijn Servaes, Dorien Glorie, Jeroen Verhaeghe, Leonie wyffels, Sigrid Stroobants, Steven Staelens

ABSTRACT:

We applied molecular brain imaging in the quinpirole rat model for compulsive checking in OCD thereby visualizing neuronal activity with FDG microPET/CT.
Animals (n = 30) received either saline (CTRL; 1 mL/kg) or quinpirole (QP; dopamine D2-agonist, 0.5 mg/kg) in a single injection (acute group) or twice-weekly during 5 weeks (chronic group). Animals underwent PET/CT before exposure and again after the 1st injection (acute) or following the 10th injection in week 5 (chronic). Each injection was paired with an open field test and video tracking.
The QP animals displayed a strong increase in visiting frequency (checking) in both the acute (+307.49%) and the chronic group (+693.22%) compared to the control animals. Acute treatment caused rather widespread significant ($p < 0.01$) increases in neuronal activity, but not in the caudate putamen. In contrast, for the chronic group, significant ($p < 0.01$) reductions were found in the caudate putamen (-19.82% ± 8.58%), as a likely consequence of D2 desensitization, but also in the hippocampus (-19.57% ± 8.20%).
OCD hence involves a dysregulation of a neural feedback loop that not only includes the cortico-striato-thalamico-cortical circuit, but also the (para)limbic regions.

Keywords:

Quinpirole, PET, FDG, Obsessive compulsive disorder, Rat

1. INTRODUCTION:

Obsessive–compulsive disorder (OCD) is a chronic, disabling psychiatric disease characterized by a lifetime prevalence of 1.1-1.8% (American Psychiatric Association 2013). OCD-patients generally suffer from intrusive, unwanted and recurrent thoughts or images (obsessions) and display repetitive ritualistic behaviors (compulsions) to reduce their anxiety. The most common symptoms include excessive hand washing (relating to a fear of contamination), repeated checking of objects or situations, and an excessive need for a certain order (referred to as 'checking' or 'counting' behavior). In OCD patients these thoughts and behaviors have become excessive, are distressing and significantly interfere with their everyday functioning (Cicek et al. 2013). The impact this disease has on patient and close relatives caused the World Health Organization (WHO) to rank it in the top 10 leading causes of disability (Veale and Roberts 2014).

Functional neuroimaging studies in OCD patients have already shown striatal dysfunction, mainly localized in the caudate nucleus (Baxter et al. 1987). This presumably leads to inefficient thalamic gating, thereby disrupting feedback to the orbitofrontal cortex and the anterior cingulate cortex (Casale et al. 2011). The majority of studies investigating the glucose metabolism have reported increases in a number of regions such as the orbitofrontal cortex, the caudate nucleus and the cingulate cortex, most notable in the anterior part (Baxter et al. 1987; Perani et al. 1995; Casale et al. 2011), further supporting this theory. Although involvement of these regions in the manifestation of OCD is beyond doubt, reports of hyperactivity have not been

consistent throughout studies (Agarwal et al. 2013; Suetens et al. 2014), making interpretation and treatment evaluation difficult. These between-study differences are likely to be explained by heterogeneities within OCD and a number of methodological differences such as group size, analysis-technique, scanning modality and whether the scan is done in rest or paired with a task. Hence, molecular imaging techniques in appropriate and well controlled animal models of OCD could help to shed light on the basal pathological mechanisms. The current available animal models are based either on pharmacological manipulation (Szechtman et al. 2001), behavioral manipulation of naturally occurring ritualistic behavior (Joel et al. 2001) and genetic modifications (Welch et al. 2007). Although none of these models are without limitations, they do play a critical role in furthering our understanding of neuroanatomical and neurochemical underpinnings of the OC-spectrum. Furthermore they help to account for the brain mechanisms by which existing treatments such as psychotherapy, pharmacotherapy and deep brain stimulation, exert their effects on patients. Finally they are a valuable addition for the search for novel treatments (Camilla d'Angelo et al. 2014). Several studies have thoroughly investigated the validity of these models (Szechtman et al. 1998; Winter et al. 2007; Mundt et al. 2009; Camilla d'Angelo et al. 2014), focusing on behavioral evaluation of different treatments that have proven effective in clinical studies (Aouizerate et al. 2004; Mallet et al. 2008; Denys et al. 2010). In one of these models, the quinpirole (QP) model, rats chronically receive injections with the dopamine D2/D3 receptor agonist QP, thereby developing compulsive-like behavior resembling the compulsive checking spectrum of OCD patients (Camilla d'Angelo 2014). Compared to

68 control rats, QP rats return to a specific location excessively, often extremely rapidly,
69 and visit fewer places before returning to this location (Szechtman et al. 1998a; Winter
70 et al. 2007; Mundt et al. 2009).

71 Despite the extensive amount of behavioral studies done with this model (Winter et al.
72 2007; Zadicario et al. 2007; De Carolis et al. 2011; Haas et al. 2011; Eagle et al. 2014), no
73 in vivo imaging data is currently available. Preclinical molecular imaging is a sensitive in
74 vivo imaging tool that is currently used in preclinical research to get a deeper
75 understanding of the underlying neurobiology in a variety of neurological disorders by
76 measuring neuroreceptor kinetics with picomolar sensitivity. The use of molecular
77 imaging in an animal model for OCD enables the assessment of multiple regions
78 contributing to this specific behavior, which will assist us in unraveling the underlying
79 basic pathological networks.

80 ## 2. MATERIALS AND METHODS

81 ### *2.1. Animals*

82 The present study was carried out in accordance with the European Communities
83 Council Directive of November 24th, 1986 (86/609/EEC) for care of laboratory animals
84 and was approved by the local ethical committee (University of Antwerp under number
85 2014-18). All efforts were made to minimize suffering and to reduce the number of
86 animals. Thirty (n=30) naïve male Sprague Dawley rats (Janvier, France, 285-550 g during
87 the experiment) were housed in a temperature- and humidity-controlled vivarium in

IVC-cages with a 12-hour light-dark cycle (lights on: 8am – 8pm). All experiments were performed during daytime. Food and water were available ad libitum.

2.2. Experimental design

Prior to induction of the model, animals were handled for 2 minutes during 5 consecutive days as a habituation period. After this period animals were divided into 2 groups with each group subdivided in 2 different conditions: a control condition (CTRL), receiving saline, and a treatment condition, receiving QP. Both conditions in the first group (n = 8 x 2) would only receive an acute injection of either saline or drug, while the two conditions in the other group (n = 7 x 2) would be exposed to chronic injections of either saline or drug.

Before exposure to either the CTRL or QP condition, animals from both the acute and chronic group received a baseline [18F]-FDG PET scan. Then, as shown in Figure 1, animals were introduced to the model, receiving a first subcutaneous injection of either QP (0.5 mg/kg, dissolved in saline at a concentration of 0.5 mg/mL) or saline (1 mL/kg). Fifteen minutes after this injection, individual animals were placed on an open field (OF) for 30 minutes whereby their behavior was continuously recorded using a Basler Ace Color GigE Camera acA1300-60gc (Edmund Optics Inc., Barrington, USA). The open field was a black table (160 x 160 cm and 60 cm high), which was subdivided into 25 squares or locales. It was equipped with 4 different Plexiglas boxes (8x8x8 cm) at predefined locations (Szechtman et al. 1998b). A computer that was linked to the video camera was used to automatically monitor and score the behavior (Ethovision XT, Noldus, The

Netherlands). The total distance that was traveled as well as the frequency of visits at each open field locale was analyzed. The locale that displayed the highest frequency of visits was defined as the animal's home base (HB). In addition, since an increased frequency of visits is correlated with an increased locomotion, an arithmetic was applied to assess checking behavior separate from locomotion following the method earlier described by Winter and colleagues (Winter et al. 2007). Specifically, the expected rate of return (ROR) to a certain locale was defined as the ratio of the total number of stops (checking) in one session to the total number of locales visited. Next, the number of stops at the HB was divided by this expected ROR to obtain the ratio of observed to expected ROR, which was then compared in both groups.

For the acute group, a follow-up scan was performed after the first and, for this group, only injection and associated OF-test (Figure 1). Animals from the chronic group were not scanned at that time point but continued to receive subcutaneous QP or saline injections on a twice-weekly basis, for a total of 15 injections. For these animals, a follow-up [18F]-FDG PET scan was acquired after the OF-test paired with the 10^{th} injection of either condition (in week 5, Figure 1).

For the PET scans, animals were fasted each time for a minimum of 10 hours as per the guidelines described earlier (Deleye et al. 2014). First, whole blood glucose values were measured from a drop of blood from the tail vein using a glucose meter (One Touch Ultra 2, Lifescan, France) before intravenous injection of the radiotracer. These glucose measurements were performed in duplicate, resulting in an average value. After a 1 mCi injection of [18F]-FDG-fluorodeoxyglucose ([18F]-FDG) followed by a 20-minute awake

uptake period of the tracer, the rats were anesthetized (isoflurane: 5% induction, 2% maintenance) and positioned on the µPET/CT scanner. The 20 minutes static µPET acquisition was started 30 minutes after tracer injection and was followed by a 10 minute CT-scan.

2.3. Image acquisition and processing

MicroPET/CT imaging was performed on two Siemens Inveon PET-CT scanners (Siemens Preclinical Solution, Knoxville, TN). The energy and coincidence timing window was set to 350 – 650 keV and 3.432 nsec, respectively, with a spatial resolution of 1.4 mm at the center of the field of view (FOV) (Kemp et al. 2009). The axial and transaxial FOVs are 10.0 and 12.7 cm, respectively.

The µPET images were reconstructed using 4 iterations with 16 subsets of the 2D ordered subset expectation maximization (OSEM) algorithm following Fourier rebinning. Normalization, dead time, CT-based attenuation and single-scatter stimulation scatter correction were applied. The resulted image was spatially normalized into the space of an [18F]-FDG brain template using brain normalization in PMOD v3.3 (PMOD Technologies, Switzerland) and was subsequently masked to remove any extracerebral activity. Images were then scaled for the injected dose, measured glucose values and weight, proportionally corrected for fat with the non-linear measure rSUV (rodent Standardized Uptake Value; rSUV) (Deleye et al., 2016, in revision) for each animal.

A Volume-Of-Interest-(VOI)-based analysis, using the pre-defined rat brain VOIs available from PMOD v3.3, was performed on the final images to evaluate the cross-

sectional changes in [18F]-FDG uptake between the QP group and the CTRL group both at baseline and in follow-up. Average changes in overall VOI-values are presented in table 1 with their standard deviation.

Further, as a more sensitive metric, an SPM voxel-based analysis was performed using Statistical Parametric Mapping (SPM; Welcome Department of Cognitive Neurology, London, UK) on the acquired images smoothed with a Gaussian filter of 1.5 mm in all three directions. The QP and CTRL group were compared cross-sectionally at baseline and at the follow-up time point by means of an unpaired T-test. The resulting T-maps therefore displayed hypo- or hyperactivity. For each region, the percentage significantly ($p < 0.01$) changed voxels per total VOI voxels was determined within a cluster threshold of 125 voxels (1 mm^3).

3. RESULTS

No unexpected abnormal animal behavior was recorded over the course of the experiments. Animals tolerated the dosage of QP well and no unexpected adverse effects were seen.

Average weight at baseline for the acute group was 307.57 ± 17.38 g for the CTRL condition and 326 ± 14.27 g for the QP condition. Although this difference was initially significant ($p < 0.05$), this difference disappeared at the follow up scan where animals had an average weight of 358.5 ± 11.60 g for the CTRL condition and 359 ± 7.46 g for the QP condition. Average glucose levels for the acute group at baseline were not

172 significantly different with 82.94 ± 12.32 mg/dL for CTRL condition and 69.25 ± 17.94
173 mg/dL for the QP condition. At follow up these values amounted to a significant
174 difference ($p < 0.05$) with 75.93 ± 8.67 mg/dL for the CTRL condition and 125 ± 20.43
175 mg/dL for the QP condition.

176 Average weight at the start of the experiment was 441 ± 4.91 g for the chronic CTRL
177 group and with 437 ± 4.35 g not significantly different for the chronic QP group. Both
178 steadily increased until the end of the experiment with 568 ± 12.8 g for the chronic CTRL
179 group and 557 ± 10.9 g for the chronic QP group, not significantly different. Average
180 glucose values between the chronic groups did not significantly differ at baseline (CTRL:
181 95.3 ± 5.12 mg/dl; QP: 83.3 ± 5.96 mg/dL) or at the follow-up time point (CTRL: 91.4 ±
182 7.32 mg/dL and QP: 94.8 ± 10.2 mg/dL). For both groups and both conditions, individual
183 weight and the animal specific glucose values are appropriately corrected for by rSUVglc
184 (cfr section 2.3).

185 *3.1. Open Field experiment*

186 After acute QP injection, when compared to the CTRL condition, animals traveled a
187 significantly ($p < 0.01$) larger distance (102.76 ± 27.39 m vs 41.84 ± 12.44 m) and visited
188 the HB significantly ($p < 0.01$) more frequent (47.88 ± 11.08 vs 11.75 ± 4.17). Also in the
189 chronic group, after the second injection during set up of the model, a significant
190 difference ($p < 0.01$) was found between the chronic QP and the CTRL condition in the
191 total distance traveled (130.61 ± 37.30 m vs 47.04 ± 20.37 m respectively) and in the
192 visiting frequency of the HB (75.7 ± 15.3 vs 12.4 ± 3.01) as shown in Figure 2. These

differences increased with higher injection number, while stabilizing after the 10th injection (280.80 ± 47.51 m vs 35.40 ± 16.66 m and 166 ± 31 vs 7.43 ± 5) in week 5.

When evaluating the ratio of observed to expected ROR, both in the acute and the chronic group, the QP condition showed a significantly ($p < 0.01$) higher value compared to their respective CTRL condition at the follow-up time point (Acute: 13.70 ± 2.33 vs 8.59 ± 1.64; Chronic: 10.0 ± 0.788 vs 4.29 ± 0.869) as shown in Figure 2C.

3.2. VOI-based analysis

Both for the acute and the chronic group the VOI-based analysis of the imaging data concluded that no significant differences were present at baseline between the treatment and CTRL condition. After the acute QP injection and exposure to the open field, a general increased metabolism throughout the entire brain of the animals treated with QP was detected (14.71% ± 5.91%) when compared to the CTRL animals. Increases were mostly notable in a number of cortical areas, the limbic system and part of the hindbrain as shown on Figure 3 and listed in Table 1. In contrast to this acute group, [18F]-FDG uptake was globally decreased (-15.49% ± 8.87%) in the QP condition for the chronic group at follow-up compared to CTRL as shown in Figure 3. Significant differences ($p < 0.05$) were found in the caudate putamen and the anterodorsal hippocampus as specified in Table 1.

3.3. Voxel-based analysis

Voxel-based analysis revealed that both the acute group and the chronic group showed

no noticeable changes in the regions of interest when comparing cross-sectionally at baseline. After the acute QP injection, 29.83% of the total brain showed a significantly ($p < 0.01$) increased metabolism, compared to the control condition, particularly in several cortical areas, the amygdala, hypothalamus and the hindbrain (Figure 4), as is summarized in Table 2. In contrast, for the chronic group at follow-up the QP condition showed a significantly ($p < 0.01$) decreased metabolism (Figure 5) compared to the CTRL condition, specifically in the caudate putamen and hippocampus as summarized in Table 2.

4. Discussion

This study describes the first in vivo imaging experiment of the QP-sensitization model. In accordance with the originally described behavior by Szechtman et al, we found that both animals acutely and chronically treated with QP display an increase in overall locomotor behavior, increasing with each injection (Szechtman et al. 1998b). Previously it has been shown that, in addition to a general increase in activity, a certain pattern emerges whereby animals visit a location of preference (HB) excessively, in a particular order and with a faster return time (Haas et al. 2011). These findings were confirmed by this study as both the frequency of HB visits and the ROR to the HB indicate a strong increase when compared to the CTRL animals, increasing with the number of injections. CTRL animals treated with saline did not show this remarkable difference for either parameter. Although this in itself does not indicate the establishment of the OCD pathology, the basic characteristics of non-goal directed compulsive behavior appear to

234 be intrinsic to this model. Nonetheless it should be kept in mind that compulsive
235 checking is not representative for the entire spectrum of OCD as it has previously been
236 shown that different symptoms in the pathology are likely to be linked to distinct neural
237 substrates (Alonso et al. 2013; Alonso et al. 2015).

238 Regarding the imaging data, a clear and significant metabolic increase was detected
239 after an acute injection of QP. These results point towards an initial activation of the D2-
240 receptor by QP, resulting in inhibition of the indirect pathway and associated activation
241 of the associated areas. Similarly, two studies revealed that acute administration of
242 bromocriptine, another D2-receptor agonist, increased the signal intensity, describing
243 changes in the thalamus, hypothalamus, parietal cortex, somatosensory cortex,
244 brainstem nuclei and the cerebellum (Hagino et al., 1998; Pizzolato et al., 1985). As was
245 the case with acute QP injection, both these studies also reported no significant changes
246 in the caudate-putamen after acute injection of bromocriptine, suggesting that acute
247 administration increased the local cerebral glucose uptake in regions with poor direct
248 connection to the dopaminergic system (Hagino et al., 1998). Also in line with our
249 findings, an acute injection of a D2 antagonist haloperidol caused a widespread
250 decreased metabolism (Hagino et al., 1998; Pizzolato et al., 1987) and therefore, as
251 expected, produced an opposite effect to that of the acute administration of the D2
252 agonist, QP, that is used in this study. An acute injection of sulipride, another D2
253 antagonist, caused an initial decrease in LCGU at 1h after drug administration but
254 subsequently also an increase at 3h after administration (Pizzolato et al., 1987).
255 However, existing literature is not always consistent, as an acute injection of QP has also

been reported to result in a decreased local cerebral glucose uptake in the striatum, lateral habenula and motor cortex (Carpenter et al., 2003). Differences in dose, route of administration, rat strains, type of anesthesia, recovery time and the use of freely moving versus restrained rats could possibly account for the differences.

In contrast to the metabolic increases seen after one injection, the chronic exposure revealed strong significant metabolic reductions most notably in the core of the cortico-striato-thalamico-cortical circuit, the caudate putamen, presumably in an attempt to regulate the initial cortical hyperactivity after acute injection. The continuous exposure to QP could lead to a desensitization of the D2-receptors targeted by the drug (Sanders et al., 2016; Haas et al., 2011). The interference coming from these regions that are preoccupied with the OCD-related processing could therefore result in the typical pattern-behavior displayed in the open field experiments (Henseler et al. 2007). Our in vivo results for the chronic condition are strikingly similar in both effect size and affected regions to the ex vivo autoradiography data reported previously (Carpenter et al. 2003) for a similar sensitized setup. Finally, QP has an effect on the overall energy metabolism, affecting glucose uptake in the neuronal cells (Coscina et al. 1998), which may therefore also influence the results.

Although clinical studies generally report hyperactivity in the associated brain regions of OCD patients (Casale et al. 2011; Agarwal et al. 2013; Via et al. 2014), this seems not to be a consistent finding throughout the clinical literature (Agarwal et al. 2013; Suetens et al. 2014). In clinical studies, the wide variety of patients, regarding differences in age,

277 previous treatments and medical history can significantly influence the results.

278 Besides the clear indication of involvement of the cortico-striato-thalamico-cortical-
279 circuit within the pathophysiology of OCD, other regions displayed remarkable changes
280 as well. For instance, the hippocampus, a region that has previously been suggested to
281 play a role in OCD (Kwon et al., 2003), in particular regarding its cognitive deficit
282 dimension, was decreased in metabolic activity after chronic exposure to QP. More
283 recently, preclinical results have revealed that lesions in the hippocampal regions can
284 cause a perseveration of certain behaviors (Kosaki and Watanabe, 2012; Chudasama et
285 al 2012). Also in another model for compulsive behavior, characterized by the
286 contrafreeloading of water that is induced by pramipexole (D3-agonist), a significant
287 decrease in hippocampal long-term potentiation (LTP) was found (Schepisi et al. 2015)
288 Additionally, lower ratios of N-acetyl-l-aspartate/choline (NAA/CHO) were found in OCD
289 patients when compared to healthy controls (Atmaca et al. 2009) in the hippocampus.
290 The involvement of the hippocampus in tasks such as spatial memory and navigation,
291 together with its direct projections to the OFC provide further explanation for the
292 particular behavior these animals display.

293 Another region in the limbic system, the amygdala, which is a key structure in fear
294 processing, has been implied to be of importance in the pathophysiology of OCD (Milad
295 and Rauch 2011) as amygdala-centric processes could have a substantial role in the
296 symptom dimensions of OCD related to abnormal fear processing (Via et al. 2014). Our
297 results showed that this region was characterized by a decreased metabolic activity

298 after chronic exposure to QP. Several clinical reports have previously suggested that the
299 amygdala's responsivity is attenuated in OCD patients regarding facial recognition and
300 non-disorder-specific stimuli (Cannistraro et al. 2004; Britton et al. 2010), further
301 implying involvement of the amygdala in the disease's pathophysiology. Together with
302 the decreases in hippocampus and the closely associated entorhinal cortex, this points
303 towards a decreased connectivity of limbic regions, which may be related to several
304 neurocognitive deficits observed in OCD patients involving implicit learning, emotion
305 processing and expectation, and processing of reward and punishment (Göttlich et al.
306 2014). This limbic disconnection from the fronto-parietal regions might explain why
307 intrusive thoughts are threatening to patients but not to healthy subjects (Göttlich et al.
308 2014).

309 In order to confirm our findings and to assess the stability of the model, the chronic
310 animal model and CTRL group were maintained by QP and saline injections to perform
311 an additional follow-up scan after the 15^{th} injection and open field test. These additional
312 measurements (data not shown) confirmed these findings.

313 In summary, chronical injections with QP induce a compulsive checking behavior that
314 resembles human compulsive behavior. Due to significant decreases in striatal and
315 cortical regions, our results indicate the involvement of the cortico-striato-thalamico-
316 cortical circuit in the pathophysiology of this OCD-model, leading to inefficient thalamic
317 gating (Casale et al. 2011). As initial exposure to QP results in increased metabolism,
318 chronic administration might therefore be a consequence of the desensitization of the

receptors targeted by the drug in the dopaminergic regions. Alterations in other key structures as the amygdala, hippocampus and entorhinal cortex, which are directly involved in memory and fear processing, point towards a more extensive disease mechanism. These findings thereby support the hypothesis that the pathophysiology of OCD, more specifically concerning the compulsive checking behavior, involves a dysregulation of a neural feedback circuit that not only includes the cortical and striatal structures, but also the (para)limbic regions. Future work should investigate the cause of this dysregulation and the underlying brain neurochemistry on a molecular level. A next, valuable step in this research could therefore be the evaluation of neurotransmitters involved, such as dopamine and glutamate, after acute and chronic administration of QP in the rat model by molecular imaging.

ACKNOWLEDGEMENTS

This work was funded by Antwerp University, Belgium through a PhD grant for S. Servaes and D. Glorie, an assistant professor position for J. Verhaeghe and L. wyffels, an associate professor position for S. Staelens and a full professor position for S. Stroobants. S. Stroobants is also supported by Antwerp University Hospital, Belgium through a departmental position. Hardware and experimental costs were supported by a DOCPRO (41/FA020000/FFB140317) of Antwerp University and a National Fund for Scientific Research Grant (42/FA020000/685). No funding sources had a role in the study design or in the collection, analysis and interpretation of the data.

The authors would like to thank Philippe Joye and Caroline Berghmans for their expertise and technical assistance.

REFERENCES

Agarwal, S., Jose, D., Baruah, U., Shivakumar, V., Kalmady, S., Venkatasubramanian, G., Mataix-Cols, D., Reddy, Y., 2013. Neurohemodynamic Correlates of Washing Symptoms in Obsessive-compulsive Disorder: A Pilot fMRI Study Using Symptom Provocation Paradigm. Indian J. Psychol. Med. 35(1), 67–74.

Alonso, P., Orbegozo, A., Pujol, J., López-Solà, C., Fullana, M.À., Segalàs, C., Real, E., Subirà, M., Martínez-Zalacaín, I., Menchón, J.M., Harrison, B.J., Cardoner, N., Soriano-Mas, C., 2013. Neural correlates of obsessive-compulsive related dysfunctional beliefs. Prog. Neuropsychopharmacol. Biol. Psychiatry 47, 25–32.

Alonso, P., Lopez-Sola, C., Real, E., Segalas, C., Menchon, J.M., 2015. Animal models of obsessive – compulsive disorder : utility and limitations. Neuropsychiatr. Dis. Treat. 11, 1939–1955.

American Association, 2013. Diagnostic and Statistical Manual of Mental Disorders (DSM-5®).

Aouizerate, B., Guehl, D., Cuny, E., Rougier, A., Bioulac, B., Tignol, J., Burbaud, P., 2004. Pathophysiology of obsessive--compulsive disorder. Prog. Neurobiol. 72(3), 195–221.

Atmaca, M., Yildirim, H., Ozdemir, H., Koc, M., Ozler, S., Tezcan, E., 2009. Neurochemistry of the hippocampus in patients with obsessive-compulsive disorder. Psychiatry Clin Neurosci 63, 486–490.

Baxter, L., Phelps, M., Mazziotta, J., Guze, B., Schwartz, J., Selin, C., 1987. Local cerebral glucose metabolic rates in obsessive-compulsive disorder. A comparison with rates in unipolar depression and in normal controls. Arch. Gen. Psychiat. 44(3), 211–8.

Britton, J., Stewart, S., Killgore, W., Rosso, I., Price, L., Gold, A., Pine, D., Wilhelm, S., Jenike, M., Rauch, S., 2010. Amygdala activation in response to facial expressions in pediatric obsessive-compulsive disorder. Depress. Anxiety. 27(7), 643–51.

Camilla d'Angelo, L.-S., Eagle, D.M., Grant, J.E., Fineberg, N.A., Robbins, T.W., Chamberlain, S.R., 2014. Animal models of obsessive-compulsive spectrum disorders. CNS Spectr. 19, 28–49.

Cannistraro, P., Wright, C., Wedig, M., Martis, B., Shin, L., Wilhelm, S., Rauch, S., 2004. Amygdala responses to human faces in obsessive-compulsive disorder. Biol. Psychiat. 56(12), 916–20.

Carpenter, T.L., Pazdernik, T.L., Levant, B., 2003. Differences in quinpirole-induced local cerebral glucose utilization between naive and sensitized rats. Brain Res. 964(2), 295–301.

Casale, A., Kotzalidis, G., Rapinesi, C., Serata, D., Ambrosi, E., Simonetti, A., Pompili, M., Ferracuti, S., Tatarelli, R., Girardi, P., 2011. Functional Neuroimaging in Obsessive-Compulsive Disorder. Neuropsychobiol. 64(2), 61–85.

Chudasama, Y., Doobay, V.M., Liu, Y., 2012. Hippocampal-Prefrontal Cortical Circuit Mediates Inhibitory Response Control in the Rat. J. Neurosci. 32, 10915–10924.

Cicek, E., Cicek, I., Kayhan, F., Uguz, F., Kaya, N., 2013. Quality of life, family burden and associated factors in relatives with obsessive--compulsive disorder. Gen. Hosp. Psychiat. 35(3), 253–8.

Coscina, D.V., Currie, P.J., Szechtman, H., 1998. Association of altered whole-body metabolism with locomotor sensitization induced by quinpirole. Physiol. Behav. 63(5), 755–61.

De Carolis, L., Schepisi, C., Milella, M., Nencini, P., 2011. Clomipramine, but not haloperidol or aripiprazole, inhibits quinpirole-induced water contrafreeloading, a putative animal model of compulsive behavior. Psychopharmacol. 218(4), 749–59.

Deleye, S., Verhaeghe, J., wyffels, L., Dedeurwaerdere, S., Stroobants, S., Staelens, S., 2014. Towards a reproducible protocol for repetitive and semi-quantitative rat brain imaging with (18) F-FDG: exemplified in a memantine pharmacological challenge. NeuroImage. 96, 276–87.

Deleye, S., Verhaeghe, J., Stroobants, S., Staelens, S., 2016. rSUV: an uptake value standardised for rats to more accurately quantify 18F-FDG brain uptake. J. Cereb. Blood Flow Metab., submitted 13/04/2016.

Denys, D., Mantione, M., Figee, M., Munckhof, P., Koerselman, F., Westenberg, H., Bosch, A., Schuurman, R., 2010. Deep brain stimulation of the nucleus accumbens for treatment-refractory obsessive-compulsive disorder. Arch. Gen. Psychiat. 67(10), 1061–8.

Eagle, D., Noschang, C., Camilla D'Angelo, L.-S., Noble, C., Day, J., Dongelmans, M., Theobald, D., Mar, A., Urcelay, G., Morein-Zamir, S., Robbins, T., 2014. The dopamine D2/D3 receptor agonist quinpirole increases checking-like behaviour in an operant observing response task with uncertain reinforcement: a novel possible model of OCD. Behav. Brain Res. 264, 207–229.

Göttlich, M., Krämer, U.M., Kordon, A., Hohagen, F., Zurowski, B., 2014. Decreased limbic and increased fronto-parietal connectivity in unmedicated patients with obsessive-compulsive disorder. Hum. Brain Mapp. 35, 5617–5632.

Haas, R., Nijdam, A., Westra, T., Kas, M., Westenberg, H., 2011. Behavioral pattern analysis and dopamine release in quinpirole-induced repetitive behavior in rats. J. Psychopharmacol. 25(12), 1712–9.

Hall, H., Sedvall, G., Magnusson, O., Kopp, J., Halldin, C., Farde, L., 1994. Distribution of D1- and D2-dopamine receptors, and dopamine and its metabolites in the human brain. Neuropsychopharmacol. 11(4), 245–56.

Hagino, H., Tabuchi, E., Kurachi, M., Saitoh, O., Sun, Y., Kondoh, T., Ono, T., Torii, K., 1998. Effects of D2 dopamine receptor agonist and antagonist on brain activity in the rat assessed by functional magnetic resonance imaging. Brain Res. 813, 367–73.

Henseler, I., Gruber, O., Kraft, S., Krick, C., Reith, W., Falkai, P., 2007. Compensatory hyperactivations as markers of latent working memory dysfunctions in patients with obsessive-compulsive disorder: an fMRI study. J. Psychiatry Neurosci. 33(3), 209–15.

Joel, D., Avisar, A., Doljansky, J., 2001. Enhancement of excessive lever-pressing after post-training signal attenuation in rats by repeated administration of the D1 antagonist SCH 23390 or the D2 agonist quinpirole, but not the D1 agonist SKF 38393 or the D2 antagonist haloperidol. Behav. Neurosci. 115(6), 1291–300.

Kemp, B.J., Hruska, C.B., McFarland, A.R., Lenox, M.W., Lowe, V.J., 2009. NEMA NU 2-2007 performance measurements of the Siemens Inveon preclinical small animal PET system. Phys. Med. Biol. 54(8), 2359–76.

Kosaki, Y., Watanabe, S., 2012. Dissociable roles of the medial prefrontal cortex, the anterior cingulate cortex, and the hippocampus in behavioural flexibility revealed by serial reversal of three-choice discrimination in rats. Behav. Brain Res. 227, 81–90.

Kwon, J.S., Shin, Y.-W., Kim, C.-W., Kim, Y.I., Youn, T., Han, M.H., Chang, K.-H., Kim, J.-J., 2003. Similarity and disparity of obsessive-compulsive disorder and schizophrenia in MR volumetric abnormalities of the hippocampus-amygdala complex. J. Neurol. Neurosurg. Psychiatry 74, 962–964.

Mallet, L., Polosan, M., Jaafari, N., Baup, N., Welter, M.-L., Fontaine, D., Montcel, S., Yelnik, J., Chéreau, I., Arbus, C., Raoul, S., Aouizerate, B., Damier, P., Chabardès, S., Czernecki, V., Ardouin, C., Krebs, M.-O., Bardinet, E., Chaynes, P., Burbaud, P., Cornu, P., Derost, P., Bougerol, T., Bataille, B., Mattei, V., Dormont, D., Devaux, B., Vérin, M., Houeto, J.-L., Pollak, P., Benabid, A.-L., Agid, Y., Krack, P., Millet, B., Pelissolo, A., 2008. Subthalamic Nucleus Stimulation in Severe Obsessive--Compulsive Disorder. New Engl. J. Med. 359(20), 2121–34.

Milad, M., Rauch, S., 2011. Obsessive-compulsive disorder: beyond segregated cortico-striatal pathways. Trends Cogn. Sci. 16(1), 43–51.

Mundt, A., Klein, J., Joel, D., Heinz, A., Djodari-Irani, A., Harnack, D., Kupsch, A., Orawa, H., Juckel, G., Morgenstern, R., Winter, C., 2009. High-frequency stimulation of the nucleus accumbens core and shell reduces quinpirole-induced compulsive checking in rats. Eur. J. Neurosci. 29(12), 2401–12.

Narendran, R., Mason, S.N., Chen, C., Himes, M., Keating, P., May, M.A., Rabiner, E.A., Laruelle, M., Mathis, C.A., Frankle, G.W., 2011. Evaluation of dopamine D2/3specific binding in the cerebellum for the positron emission tomography radiotracer [11C]FLB 457: Implications for measuring cortical dopamine release. Synapse. 65(10), 991–7.

Perani, D., Colombo, C., Bressi, S., Bonfanti, A., Grassi, F., Scarone, S., Bellodi, L., Smeraldi, E., Fazio, F., 1995. [18F]FDG PET study in obsessive-compulsive disorder. A clinical/metabolic correlation study after treatment. Brit. J. Psychiat. 166(2), 244–50.

Pizzolato, G., Soncrant, T.T., Rapoport, S.I., 1985. Time-course and regional distribution of the metabolic effects of bromocriptine in the rat brain. Brain Res. 341, 303–312.

458 Pizzolato, G., Soncrant, T.T., Larson, D.M., Rapoport, S.I., 1987. Stimulatory effect of the
459 D2 antagonist sulpiride on glucose utilization in dopaminergic regions of rat brain. J.
460 Neurochem. 49, 631–638.

461 Sander, C.Y., Hooker, J.M., Catana, C., Rosen, B.R., Mandeville, J.B., 2015. Imaging
462 Agonist-Induced D2/D3 Receptor Desensitization and Internalization In Vivo with
463 PET/fMRI. Neuropsychopharmacology 41, 1–10.

464 Schepisi, C., Pignataro, A., Doronzio, S.S., Piccinin, S., Ferraina, C., Di Prisco, S., Feligioni,
465 M., Pittaluga, A., Mercuri, N.B., Ammassari-Teule, M., Nisticò, R., Nencini, P., 2015.
466 Inhibition of hippocampal plasticity in rats performing contrafreeloading for water
467 under repeated administrations of pramipexole. Psychopharmacol. doi:10.1007/s00213-
468 015-4150-4

469 Suetens, K., Nuttin, B., Gabriëls, L., Laere, K., 2014. Differences in Metabolic Network
470 Modulation Between Capsulotomy and Deep-Brain Stimulation for Refractory
471 Obsessive-Compulsive Disorder. J. Nuc. Med. 55(6), 951959.

472 Szechtman, H., Eckert, M., Tse, W., Boersma, J., Bonura, C., McClelland, J., Culver, K.,
473 Eilam, D., 2001. Compulsive checking behavior of quinpirole-sensitized rats as an animal
474 model of Obsessive-Compulsive Disorder(OCD): form and control. BMC Neurosci. 2(1), 4.

475 Szechtman, H., Sulis, W., Eilam, D., 1998 a. Quinpirole induces compulsive checking
476 behavior in rats: a potential animal model of obsessive-compulsive disorder (OCD).
477 Behav. Neurosci. 112(6), 1475.

478 Szechtman, H., Sulis, W., Eilam, D., 1998 b. Quinpirole induces compulsive checking
479 behavior in rats: a potential animal model of obsessive-compulsive disorder (OCD).
480 Behav. Neurosci. 112(6), 1475–85.

481 Veale, D., Roberts, A., 2014. Obsessive-compulsive disorder. BMJ. 348, g2183.

482 Via, E., Cardoner, N., Pujol, J., Alonso, P., Lopez-Sola, M., Real, E., Contreras-Rodriguez,
483 O., Deus, J., Segalas, C., Menchon, J., Soriano-Mas, C., Harrison, B., 2014. Amygdala
484 activation and symptom dimensions in obsessive-compulsive disorder. Brit. J. Psychiat.
485 204(1), 61–8.

486 Welch, J., Lu, J., Rodriguiz, R., Trotta, N., Peca, J., Ding, J.-D., Feliciano, C., Chen, M.,
487 Adams, J., Luo, J., Dudek, S., Weinberg, R., Calakos, N., Wetsel, W., Feng, G., 2007.
488 Cortico-striatal synaptic defects and OCD-like behaviours in Sapap3-mutant mice.
489 Nature. 448(7156), 894–900.

490 Winter, C., Mundt, A., Jalali, R., Joel, D., Harnack, D., Morgenstern, R., Juckel, G., Kupsch,
491 A., 2007. High frequency stimulation and temporary inactivation of the subthalamic
492 nucleus reduce quinpirole-induced compulsive checking behavior in rats. Exp. Neurol.
493 210(1), 217–28.

494 Zadicario, P., Ronen, S., Eilam, D., 2007. Modulation of quinpirole-induced compulsive-
495 like behavior in rats by environmental changes: Implications for OCD rituals and for
496 exploration and navigation. BMC Neurosci. 8(1), 23.

FIGURES AND TABLES

REGION	ACUTE			CHRONIC		
	Cross-sectional % change			Cross-sectional % change		
	mean	std		mean	std	
AcbCore/Shell	10.97%	5.17%		-17.41%	8.72%	
Amygdala	15.28%	6.61%	*	-17.78%	8.55%	
CaudatePutamen	10.71%	5.53%		-19.82%	8.58%	*
CortexAuditory	12.62%	5.91%		-16.85%	8.61%	
CortexCingulate	11.16%	5.37%	*	-17.31%	9.25%	
CortexEntorhinal	16.97%	6.03%		-17.53%	8.56%	
CortexFrontal	6.67%	6.81%		-17.37%	9.35%	
CortexInsular	15.20%	6.07%	*	-15.66%	8.78%	
CortexMedialPrefrontal	11.93%	5.62%		-16.62%	8.80%	
CortexMotor	10.25%	5.71%		-15.28%	9.22%	
CortexOrbitofrontal	12.69%	5.80%	*	-15.06%	8.83%	
CortexRetrosplenial	10.96%	6.21%		-15.40%	9.19%	
CortexSomatosensory	15.39%	5.61%	*	-13.50%	8.97%	
CortexVisual	8.39%	5.82%	*	-14.59%	8.77%	
HippocampusAnteroDorsal	10.72%	5.92%		-19.57%	8.20%	*
HippocampusPosterior	12.21%	6.00%		-17.95%	8.31%	
Hypothalamus	16.87%	7.22%	*	-16.89%	8.56%	
InferiorColliculus	17.46%	6.22%	*	-10.53%	9.40%	
Midbrain	17.40%	5.84%	**	-12.13%	8.70%	
Olfactory	16.55%	6.00%	*	-15.42%	8.95%	
Pituitary	24.61%	11.14%	*	-18.53%	9.14%	
Pons	20.30%	8.81%	*	-11.48%	8.61%	
SuperiorColliculus	14.81%	5.64%	*	-13.15%	9.05%	
ThalamusWhole	13.02%	5.74%	*	-16.97%	8.80%	
Ventral Tegmental Area	18.66%	6.24%	**	-14.40%	8.79%	
WholeBrain	14.71%	5.91%		-15.49%	8.87%	

Table 1 – VOI-based analysis:

A cross-sectional comparison between the quinpirole (QP) condition and the time-matched control (CTRL) condition at the follow-up timepoint is represented

here for both the acute and the chronic QP group concerning their average regional uptake values.
P-values were not corrected for multiple comparisons; * = $p < 0.05$; ** = $p < 0.01$

	ACUTE (hyper)	CHRONIC (hypo)
REGION	**Cross-sectional** $p < 0.01$ (Volume %)	**Cross-sectional** $p < 0.01$ (Volume %)
AcbCore/Shell	3.12%	0.00%
Amygdala	31.12%	2.10%
CaudatePutamen	4.28%	5.11%
CortexAuditory	6.60%	0.87%
CortexCingulate	4.34%	0.00%
CortexEntorhinal	40.86%	8.39%
CortexInsular	11.66%	0.00%
CortexMedialPrefrontal	0.00%	0.00%
CortexMotor	10.19%	0.00%
CortexOrbitofrontal	16.16%	0.00%
CortexRetrosplenial	0.25%	0.00%
CortexSomatosensory	38.84%	0.00%
CortexVisual	2.22%	0.00%
HippocampusAnteroDorsal	0.08%	11.06%
HippocampusPosterior	6.50%	3.15%
Hypothalamus	14.28%	0.00%
InferiorColliculus	62.26%	0.00%
Midbrain	87.74%	0.00%
Olfactory	48.66%	0.00%
Pons	0.92%	0.00%
SuperiorColliculus	38.79%	0.00%
ThalamusWhole	8.21%	1.21%
Ventral Tegmental Area	84.95%	0.00%
WholeBrain	29.83%	2.22%

Table 2 – Voxel-based Analysis:

Here the investigated regions and their significantly ($p < 0.01$) affected metabolic activity after voxel-analysis are displayed as a percentage of the total regional volume for both the acute and the chronic group. For both groups, comparisons are made cross-sectionally, at the follow up time point, comparing the treated condition (QP) to the control (CTRL). Please note that for the acute group the cells display clusters of voxels that are significantly increased in metabolic activity after QP, while for the chronic group the cells display the significantly decreased voxel clusters after QP.

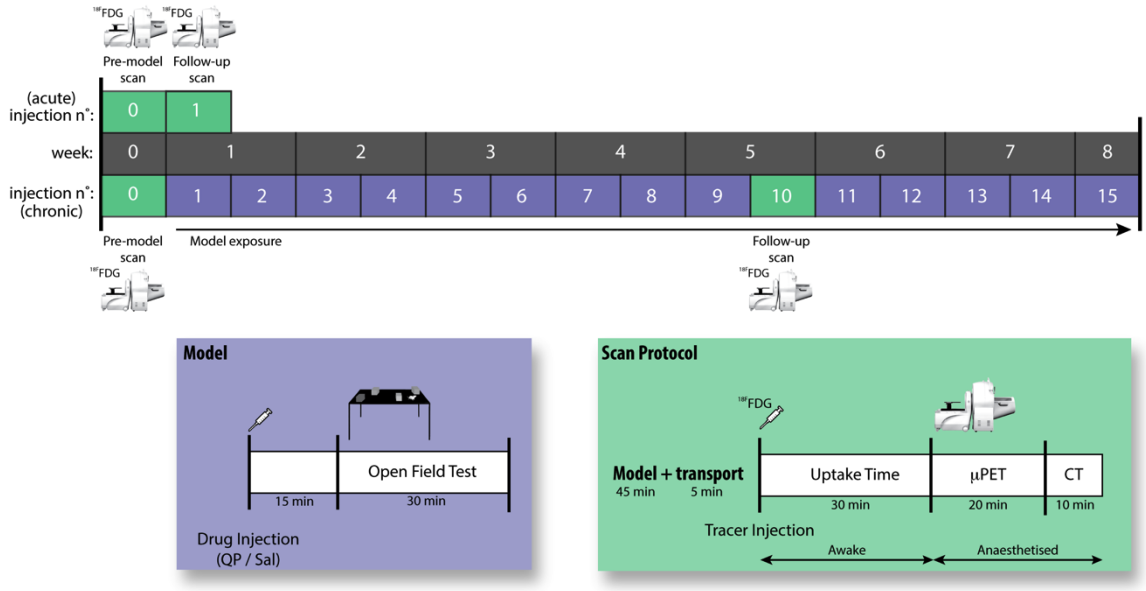

Figure 1:
Experimental protocol: a baseline [18F]-FDG scan (green) was acquired of both the acute and chronic groups before (i) an acute QP or saline injection or (ii) twice-weekly injections of either QP or saline each time paired with an open field test (blue). Further, follow-up scans (green) to stage the pathology, after the first injection for the acute group and after the 10th injection (in week 5) for the chronic group, were acquired. Finally, the chronic model was maintained by giving extra injections (11 – 15).

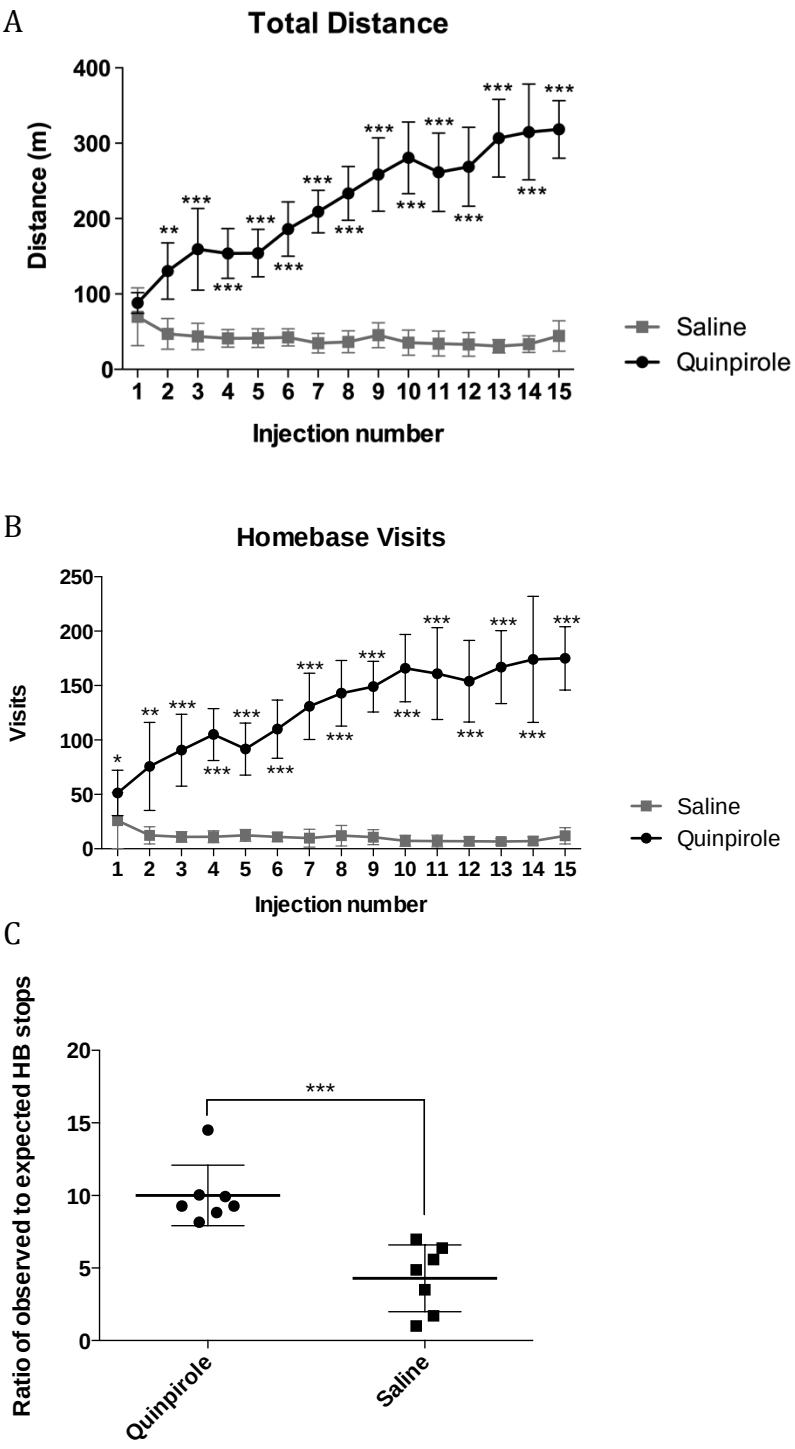

Figure 2:
During the Open Field Test, the total distance **(A)** and the number of homebase visits **(B)** were recorded. Additionally the ratio of observed-to-expected-homebase stops at the 10th injection was calculated **(C)**.

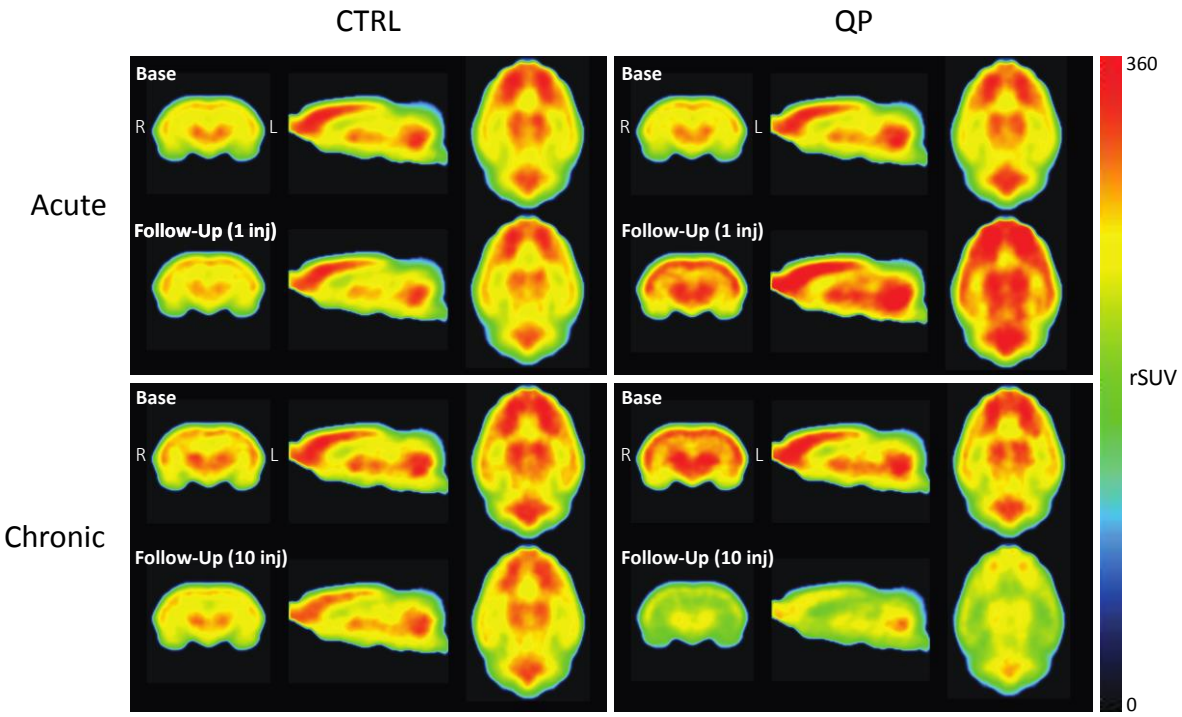

Figure 3:
18F-FDG-images, corrected for rSUV, at baseline and follow-up for both the acute and chronic group in both conditions (CTRL and QP).
CTRL - Control; QP - Quinpirole

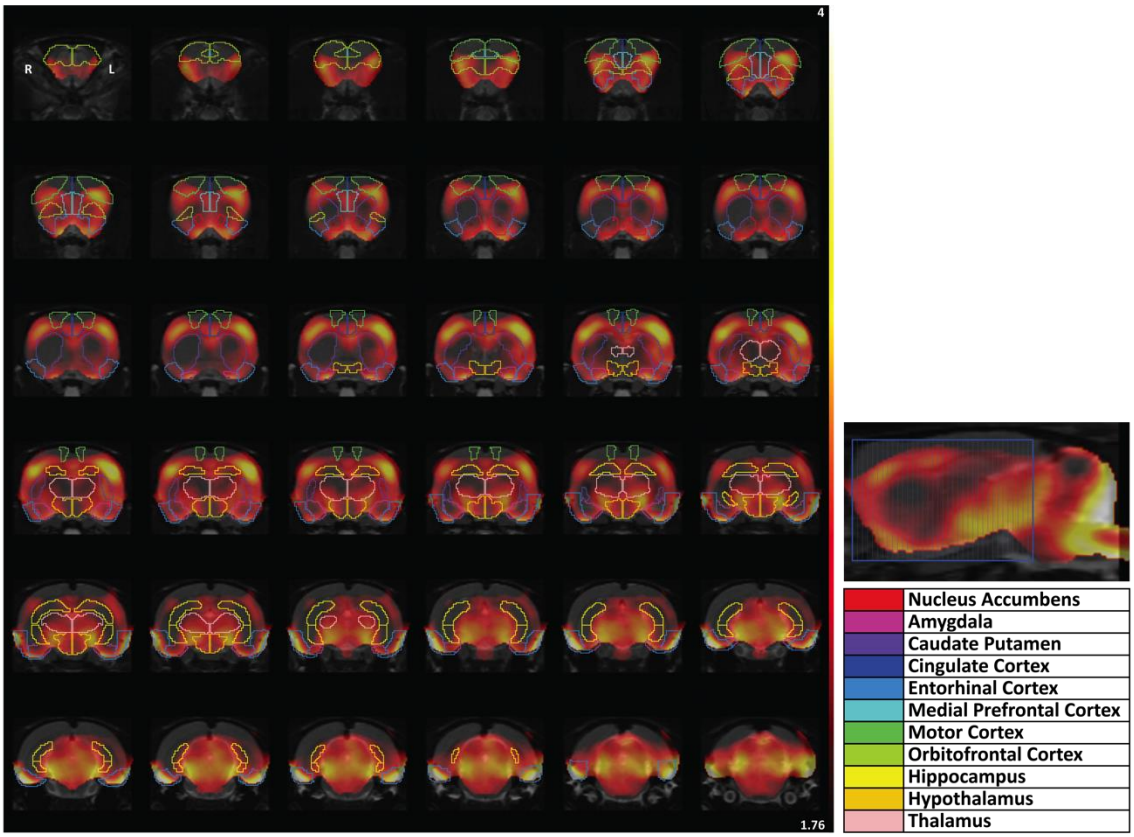

Figure 4:
Coronal slices through the brain displaying significantly changed ($p < 0.05$) voxels for the QP condition versus the CTRL animals at follow-up of the acute group (cross-sectional).

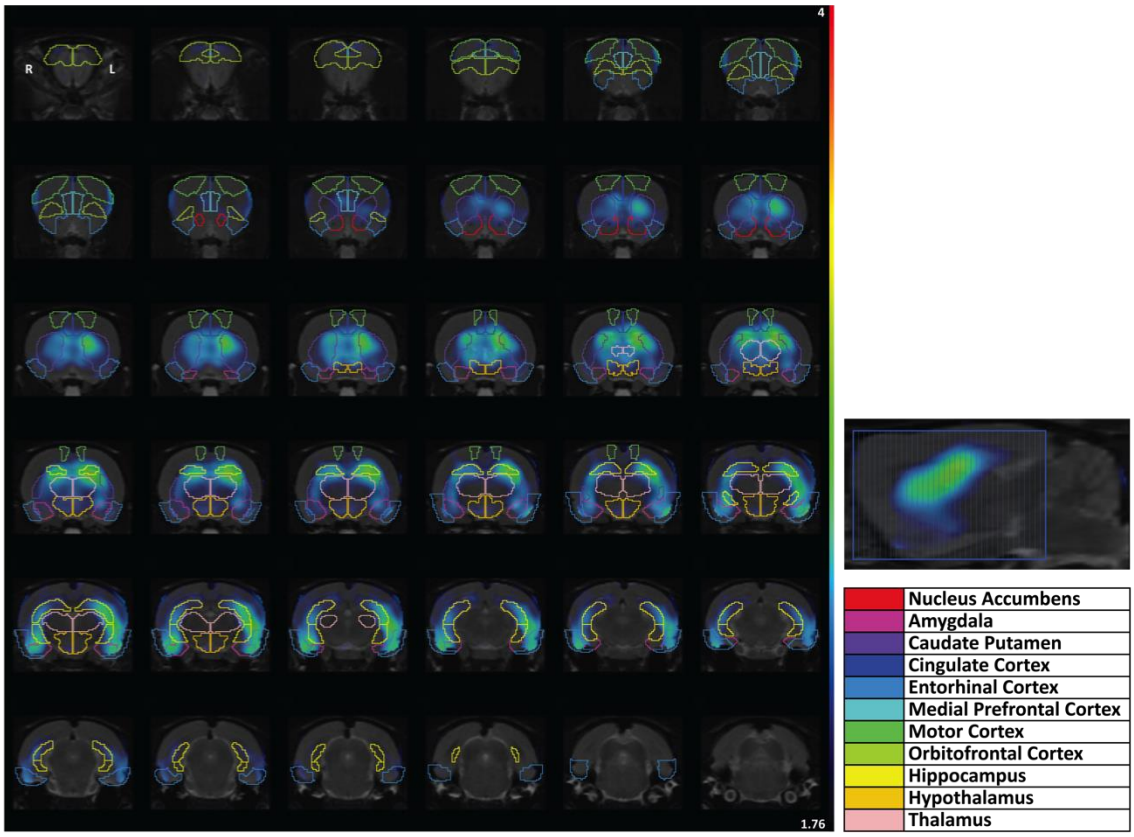

Figure 5:

Coronal slices through the brain displaying significantly changed ($p < 0.05$) voxels for the QP condition versus the CTRL animals at follow-up of the chronic group (cross-sectional).